Decay processes in microsolvated clusters : A complex absorbing potential based equation-of-motion coupled cluster investigations[†]

Ravi Kumar,[‡,¶] Aryya Ghosh,[§] and Nayana Vaval[*,¶]

‡Academy of Scientific and Innovative Research, CSIR-Human Resource Development Center (CSIR-HRDC) Campus, Postal Staff College Area ,Ghaziabad, Uttar Pradesh, 201002, India
¶Electronic Structure Theory Group, Physical Chemistry Division, CSIR-National Chemical Laboratory, Pune, 411008, India
§Department of Chemistry, Ashoka University, Sonipat, Haryana,131029 India

E-mail: np.vaval@ncl.res.in

Abstract

We have employed the highly accurate complex absorbing potential based ionization potential equation-of-motion coupled cluster singles and doubles (CAP-IP-EOM-CCSD) method to study the various intermolecular decay processes in ionized metals (Li^+, Na^+, K^+) microsolvated by water molecules. For the Li atom, the electron is ionized from the 1s subshell. However, for Na and K atoms, the electron is ionized from 2s and both 2s and 2p subshells, respectively. We have investigated decay processes for

---

[†]Decays in cationic alkali metals

the Li^+-$(H_2O)_n$; (n=1-3) systems as well as Na^+-$(H_2O)_n$; (n=1,2), and K^+-H_2O. The Lithium cation in water can decay only via electron transfer mediated decay (ETMD) as there are no valence electrons in Lithium. We have investigated how the various decay processes change in the presence of different alkali metal atoms and how the increasing number of water molecules play a significant role in the decay of microsolvated systems. To see the effect of the environment, we have studied the Li^+-NH_3 (in comparison to Li^+-H_2O). In the case of Na^+-H_2O, we have studied the impact of bond distance on the decay width. The effect of polarization on decay width is checked for the X^+-H_2O; X=Li, Na. We have used the PCM model to study the polarization effect. We have compared our results with the existing theoretical and experimental results wherever available in the literature.

Introduction

There are various ways in which an excited/ionized atom/molecule can relax. It can relax either via radiative processes or non-radiative decay processes. A radiative decay like fluorescence or a non-radiative process like Auger decay has been exceptionally well known for a long time. Auger spectroscopy[1] has various applications in material and surface science. In 1997, Cederbaum *et al.*[2,3] proposed a new decay mechanism for inner valence ionized/excited states, called interatomic/molecular Coulomb decay (ICD). This non-local complex relaxation process happens in atomic/molecular clusters. In the original formulation of this process, a single inner-valence hole state in an atom or molecule, which cannot decay locally via the Auger mechanism due to energetic considerations, decays through energy transfer to the neighbouring atom. This knocks out an outer valence electron from the adjacent atom or molecule. Contrary to the Auger decay process, ICD is driven by the correlation between electrons located on different species, often a few nanometers apart. The ejected ICD electrons have low energy, whose value strongly depends on the initial state and chemical nature of the neighbour. In the ICD process, two positive charges are produced in close proximity

of each other, leading to a Coulomb explosion.

Electron transfer mediated decay (ETMD)[4] is another interatomic decay process initiated by ionizing radiation. In this process, not energy but electron transfer between two sub-units acts as a mediator. In ETMD, a neighbour donates an electron to an initially ionized atom or molecule, while excess energy is transferred either to the donor or to another neighbour, which emits a secondary electron to the continuum. Li^+ has only electrons in its core orbital, so it is the best example to study the ETMD process. Being an electron transfer process, ETMD is usually considerably slower than energy transfer driven ICD process. However, it becomes a vital decay pathway in a medium if ICD is energetically forbidden. Since its original formulation, ICD has been investigated theoretically[5–7] and experimentally[8–11] in a variety of systems such as rare-gas[12,13] clusters, hydrogen bonded clusters[14] and water solutions.[15,16] It has been found that not only inner-valence ionized states may undergo ICD, but any localized electronic excitation whose energy lies above the ionization potential of a neighbour can undergo ICD. Thus, the ICD of ionized-excited, doubly ionized, or neutral-excited states of clusters have been observed and investigated theoretically. Moreover, it turns out that this decay process can be initiated not only by photons but also by energetic electrons and positive heavy ions. Experimentally, the ETMD process has been observed in rare gas clusters[17–20] and alkali doped helium droplets.[21–24] Recently, Unger *et al.*[25] have investigated the ETMD process in LiCl aqueous solution. The ETMD process has been studied theoretically in hydrogen bonded clusters.[26,27] Recently, Ghosh *et al.*[28] have investigated the ETMD process in the $HeLi_2$ cluster. Their investigation, has shown that the multi-mode nuclear dynamics play a significant role in the ETMD process. The ETMD process has also been investigated theoretically in microsolvated clusters.[29]

The high efficiency of interatomic decay processes (i.e. ICD, ETMD) makes it imperative to take these interatomic decay processes into account for proper understanding of physico-chemical phenomena induced in biological systems by ionizing radiation and related to radiation damage. First, ICD and ETMD result in the production of low energy electrons

(LEEs) through ionization of the medium. LEEs are known to be very effective in causing DNA strand breaks through the resonant dissociative attachment mechanism.[30] Second, the ionization of the medium produces genotoxic radicals such as the hydroxyl radical OH. Third, both LEE and radicals are produced locally close to where an ionizing particle initially deposits energy. If this happens close to the DNA molecule, the probability of the complex being damaged significantly increases. The feasibility of ICD and ETMD among biologically relevant species was investigated theoretically.[31,32] Microsolvated clusters with alkali metal cations serve as a model system for a natural biological system because ions can impact the intracellular and extracelluar activities, i.e. the movement of enzymes[33] and activities and conformers of proteins.[34] Na^+ and K^+ ions are the key component of the sodium-potassium pump in the human body. These ions also help to transmit the signals inside the brain.[35] The proper functioning of Na^+ and K^+ ions helps us to avoid neurological diseases.[36] Therefore, the investigation of interatomic or intermolecular decay processes in microsolvated clusters will shed light on chemistry related to radiation damage. The decay rate of the interatomic decay process specifically depends on the energy of the initially ionized or excited state. Therefore, the proper treatment of the initially ionized or excited state is necessary to calculate the lifetime of the interatomic decay process. The ionization potential equation-of-motion coupled cluster method augmented by complex absorbing potential (CAP-IP-EOM-CC) method[37–43] provides proper treatment of ionized states or excited states with the inclusion of correlation effects (dynamic and non-dynamic) as well as continuum ones. Therefore, the CAP-IP-EOM-CCSD method is promising to describe the interatomic decay process efficiently.

In this paper, we have reported the implementation of the highly correlated CAP-IP-EOM-CCSD method, which is a combination of the CAP approach and equation-of-motion coupled cluster[44–50] approach to study the ETMD decay mechanism in microsolvated Li^+-$(H_2O)_n$ (n=1,3) systems, ICD in Na^+-$(H_2O)_n$;n=1,2 and Auger decay in K^+-(H_2O). To see the effect of the environment on the decay of Li 1s state, we have chosen two iso-

electronic systems, i.e. Li^+-NH_3 and Li^+-H_2O. We compare our results with the available theoretical/experimental results wherever available. This paper is organized as follows; in Section 2, we briefly discuss the equation-of-motion coupled cluster theory along with the CAP approach. Results and discussion on them are presented in Section 3. In Section 4, we conclude our findings.
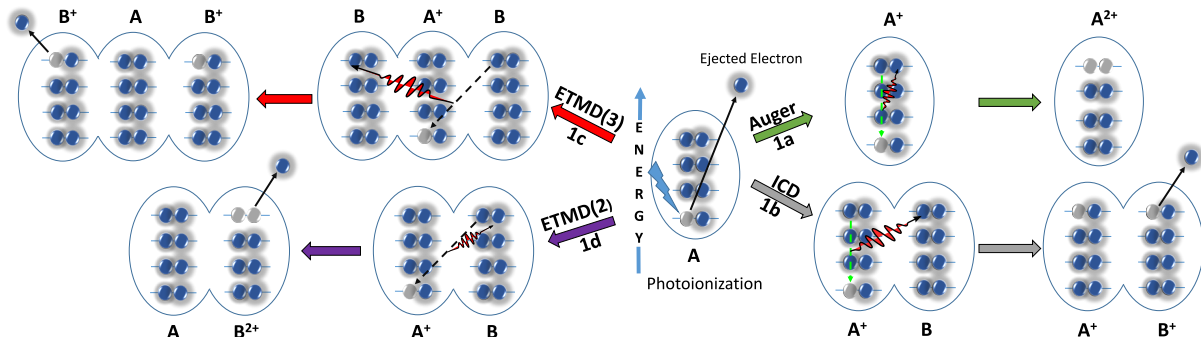
Figure 1: Various non-radiative decay processes: 1a Auger decay, 1b ICD, both 1c and 1d ETMD processes. 3 and 2 represents the number of atoms in 1c and 1d, respectively.

Theory

Complex absorbing potential based equation-of-motion coupled cluster

To calculate the position and lifetime of the decaying state, we have used the CAP-IP-EOM-CCSD method. In this section, we discuss the CAP-IP-EOM-CCSD method briefly. The decaying states are associated with the complex eigenvalues within the formulation of Siegert.[51]

$$E_{res} = E_R - i\frac{\Gamma}{2} \tag{1}$$

where E_R represents the resonance position and Γ is the decay width. The relation

5

between decay width and lifetime τ is given by

$$\tau = \frac{\hbar}{\Gamma} \tag{2}$$

The meta-stable states are not square-integrable. They can also be seen as discrete states embedded into the continuum. Hence to describe the metastable states, we require a method that can simultaneously treat electron correlation and the continuum. CAP and complex scaling[52–54] are two well-known methods used for the calculation of resonance energies. Complex absorbing potential (CAP)[54–59] along with quantum chemical methods is one of the simplest and the favoured approach. CAP has been implemented in many of the quantum chemical methods for the calculation of resonance states.[6,7,37–43,60,61] CAP along with EOM-CCSD has been used very successfully for the study of ICD and the shape resonance phenomena.

In the CAP approach, a one-particle potential $-i\eta W$ is added to the physical Hamiltonian, making the original Hamiltonian complex symmetric and non-hermitian (i.e. H(η) = H-iηW). As a result, we obtain complex eigenvalues from the CAP augmented Hamiltonian (H(η)). The real part denotes the resonance position, and the imaginary part gives half of the decay width. In H(η) = H-iηW, η represents the CAP strength, and W is a local positive-semidefinite one-particle operator. With the appropriate choice of CAP, the eigenfunctions of the complex symmetric Hamiltonian becomes square-integrable, and eigenvalues are discrete. (H(η)) is solved for various values of η. The resonance energy is obtained by diagonalizing the complex Hamiltonian matrix $H(\eta)$ for multiple values of η. The η trajectory is obtained by plotting the real part vs imaginary part of energy. The local minimum of trajectory is associated with the position and half decay width of the decaying state.

$$\nu_i(\eta) = \eta \frac{\delta E_i}{\delta \eta} \tag{3}$$

The value of η for which $\nu_i(\eta)$ is minimum gives the optimal CAP strength. We have used a box shape CAP. CAP is applied in the peripheral region so that the target remains unperturbed, yet scattered electrons are absorbed.

In the equation of motion coupled cluster approach, the target state is generated by the action of a CI-like linear operator onto the initial reference state (closed shell coupled cluster reference state). The wavefunction for the kth ionized state $|\Psi_k\rangle$ is expressed as

$$|\Psi_k\rangle = R(k)|\Phi_{cc}\rangle \tag{4}$$

where R(k) is an ionization operator. The form of the linear operator for the electron ionized state can be written as

$$R(k) = \sum_i r_i(k)i + (1/2)\sum_{ija} r_{ij}^a(k)a^\dagger ji \tag{5}$$

The reference CC wave function, $|\Phi_{cc}\rangle$ can be written as

$$|\Phi_{cc}\rangle = e^T|\Phi_0\rangle \tag{6}$$

where $|\phi_0\rangle$ is the N-electron closed shell reference determinant (restricted Hartree-Fock determinant (RHF)) and T is the cluster operator. In the coupled cluster singles and doubles (CCSD) approximation, the T operator can be defined as follows:

$$T = \sum_{ia} t_i^a a_a^+ a_i + 1/4 \sum_{ab}\sum_{ij} t_{ij}^{ab} a_a^+ a_b^+ a_i a_j \tag{7}$$

7

The indices a,b,...represent the virtual spin orbitals and the indices i,j,.. represent the occupied spin orbitals. In the IP-EOM-CCSD framework, the final ionized states are obtained by diagonalizing the coupled cluster similarity transformed Hamiltonian within a $(N - 1)$ electron space.

$$\overline{H}_N R(k)|\Phi_0\rangle = \omega_k R(k)|\Phi_0\rangle \tag{8}$$

Where

$$\overline{H}_N = e^{-T} H_N e^{T} - E_{cc} \tag{9}$$

$\overline{H}_N$ is the similarity transformed Hamiltonian and ω_k is the energy change connected with the ionization process. In the IP-EOM-CCSD approach, the matrix is generated in the 1hole and 2hole 1particle (2h-1p) subspace. Diagonalization of the matrix gives us ionization potential values.

In principle CAP can be implemented at the self consistent field (SCF)/ Hartree-Fock, coupled cluster (CC) or EOMCC level. Adding CAP at the coupled cluster level makes the cluster amplitudes complex and hence all the further calculations are complex. The N electron ground state should be unperturbed. Adding CAP at the CC or SCF level perturbs the N electron ground state itself. Then to get the correct decay width, we need to correct the N electron ground state by removing the perturbation.

$$|\Phi_{cc}(\eta)\rangle = e^{T(\eta)}|\Phi_0\rangle \tag{10}$$

$$\overline{H}_N(\eta) = e^{T(\eta)} H_N(\eta) e^{T(\eta)} - \langle\Phi_0|e^{T(\eta)} H_N(\eta) e^{T(\eta)}|\Phi_0\rangle \tag{11}$$

The resonance energy is obtained as

$$E_{res}(\eta) = \omega_k(\eta) - E_{cc}(\eta) - E_{cc}(\eta = 0) \qquad (12)$$

Thus, we lose the advantage of computing resonance energy as the direct energy difference obtained as eigenvalues of $\overline{H}_N(\eta)$ using the IP-EOM-CCSD approach. Our previous study of resonance,[62] shows that the results are not affected when we implement CAP at the IP-EOM-CCSD level. In our calculation for the decay width, we have added the CAP potential in the particle-particle block of the one-particle $\overline{H}_N$ matrix, leaving our N electron ground state unaffected. Therefore, the $\overline{H}_N(\eta)$ can be written as

$$\overline{H}_N(\eta) = e^{T(\eta=0)} H_N(\eta) e^{T(\eta=0)} - \langle \Phi_0 | e^{T(\eta=0)} H_N(\eta = 0) e^{T(\eta=0)} | \Phi_0 \rangle \qquad (13)$$

To generate the η trajectory for locating the stationary point, we need to run the CAP-IP-EOM-CCSD calculations thousands of times. We start with $\eta = 0$ and then proceed with small incremental η values. Since IP-EOM-CCSD scales as N^6, it makes our calculations computationally intensive. Convergence of the equations for various η values may be difficult as we are interested in the inner valence state, and the presence of metal ion may add to the problem. Hence we have used the full diagonalization of the matrix using BLAS routines. The dimension of the matrix usually is $NH + NH * NH * NP$ in a given basis for a system where NH and NP represent the number of occupied and unoccupied orbitals.

Results and discussion

This paper has studied the decay mechanism of the microsolvated clusters of small cations like Li^+, Na^+, K^+ with water. The bond distance, different environments and number of neighbours play an important role in the decay process. So, we have studied the behaviour of the decay width in microsolvated clusters as a function of the following parameters:

a) Effect of different molecular environments on decay width for ETMD: We have studied the decay of the Lithium 1s state in Li^+-water and Li^+-ammonia. Ammonia resembles the amino group found in bio-molecules and it is iso-electronic with water also. This is the main reason to choose these systems to study the effect of different environments on the ETMD process. b) To check the impact of an increasing number of surrounding molecules on the decay width for ETMD: We have studied the decay of the Li^+ 1s state in Li^+-$(H_2O)_n$; n=1,3. c) To see the effect of bond distance on the decay width for ICD: We have studied the decay of the 2s state of Na^+ in Na^+-H_2O at various bond lengths. The distance between sodium and oxygen is varied. d) To study the effect of polarization on the decay width, we have studied Li^+-water and Na^+-water systems in the gaseous and liquid phases. We have used the PCM model[63] to study the liquid phase.

We have studied ICD of the Sodium 2s state in Na^+-$(H_2O)_n$; n=1,2 and Auger decay of potassium 2s and 2p states in K^+-(H_2O). The details of the geometries used in this paper are available in the supporting information along with the basis set and method used for the geometry optimization. Geometries were optimized using the Gaussian09[64] software package. For the rest of the calculations, the codes used are homegrown.

Table 1: Effect of variation of basis set on decay width of the Li 1s state in Li^+-H_2O for ETMD process

Basis	Energy (eV)	Width(meV)	lifetime(fs)
aug-cc-pVDZ	72.36	11	60
aug-cc-pVDZ+F(O)	72.32	12	56
aug-cc-pVTZ	71.89	6.6	98
aug-cc-pVTZ+F(O)	72.16	7	96

Choice of basis set for ETMD process of 1s state of Li^+ in Li^+-H_2O

We have studied Li^+-water in four different basis sets. Basis-A is an aug-cc-pVDZ basis set.[65] Basis-B is constructed by adding an extra Rydberg type f function on the oxygen atom of the water molecule in Basis-A. In the Li^+-water system, after ionizing the electron from the 1s

orbital of lithium, an electron will be transferred from oxygen to fill the 1s vacancy created on lithium. The excess energy will be used to knock out a secondary electron from oxygen. Thus, it is important to have Rydberg type function on oxygen to get the continuum effect. The exponent of the f function are constructed according to the method of Kaufmann et al.[66] Basis-C is an aug-cc-pVTZ basis set.[67] Basis-D is constructed using the aug-cc-pVTZ basis set on lithium and oxygen atoms and the cc-pVTZ basis set for the hydrogen atom. In basis-D, an extra Rydberg f function is added to the oxygen atom similar to the basis-B. The CAP box side lengths are chosen to be $C_x = C_y = \delta c$ and $C_z = \delta c + R/2$ a.u. The δc value is chosen to be 5.0 a.u for the aug-cc-pVDZ basis set and 6 a.u for the aug-cc-pVTZ basis set. Table 1 reports the resonance position and decay width (lifetime) for the Lithium 1s state in all four basis sets. The triple zeta (TZ) quality basis reduces the decay position by 0.5 eV. The addition of the Rydberg f function on oxygen has minimal effect on the decay position (i.e. ionization potential) and the decay width in double zeta and triple zeta basis sets. For the Li$^+$-water dimer and trimer study, we have used basis-A (i.e. aug-cc-pVDZ basis[65]) as the method scales N^6, making it computationally expensive with the higher basis set.

Effect of different molecular environments on the ETMD process

To see the impact of different molecular environments on the decay of the lithium 1s state, we have chosen Li$^+$-NH$_3$ and Li$^+$-H$_2$O as study systems. Since they are iso-electronic systems, they are relevant systems to study the effect of different molecular environments on the decay width of lithium 1s state for the ETMD process. We have used the aug-cc-pVTZ + Rydberg 1f function on oxygen and nitrogen. The δc value chosen to be 6.0 a.u. We have presented our results in Table 2.

The ionization potential of the Li 1s state is 71.89 eV and 71.18 eV in Li$^+$-H$_2$O and Li$^+$-NH$_3$, respectively. The decay widths are 7 meV and 8 meV, respectively. The decay is faster in Li$^+$-NH$_3$ (lifetime of 81 fs) than the Li$^+$-H$_2$O (lifetime of 96 fs). It means that

11

(a) Ammonia lone pair   (b)Water lone pair
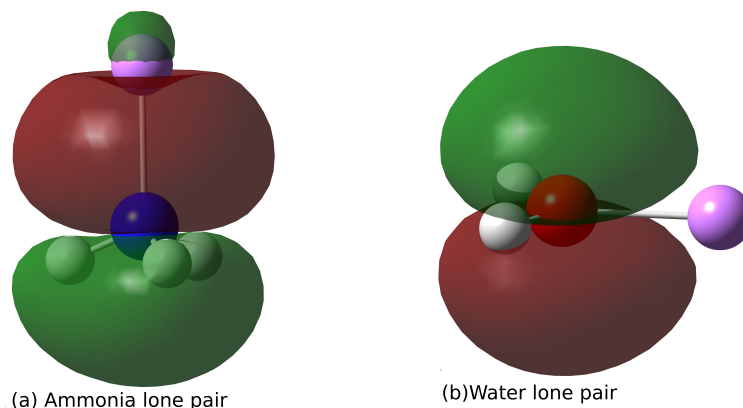
Figure 2: a) Orientation of lone pair in Li^+-NH_3 is toward Li atom, making electron transfer easier, hence a shorter lifetime. b) The direction of lone pair in Li^+-H_2O is perpendicular to the molecular plane, making electron transfer difficult, thus more significant lifetime. Above picture is generated for isosurface value 0.02 $e\mathring{A}^{-3}$. Atom colour code Pink: Lithium, Blue: Nitrogen, Red: Oxygen, and White: Hydrogen.

the transfer of the electron to the 1s vacant position of the Li atom is faster in the case of ammonia than water. It can be explained on the following basis a.) Electronegativity: Oxygen is a more electronegative atom than nitrogen, making the electron transfer slower in case of water than ammonia. b.) Position of lone pair electron: The position of the lone pair electron in the Li^+-NH_3 is between Li^+ and nitrogen. In Li^+-H_2O, the position of lone pair is perpendicular to Li^+-H_2O molecular plane (not in between Li^+ and oxygen); see figure-2. Because of the directional nature of the p-orbital and lone pair's orientation toward lithium, electron transfer is much faster in case of ammonia than water. Orbitals of figure-2 are generated by Gaussian09[64] software package using density functional theory with B3LYP functional[68-71] and aug-cc-pVTZ basis set.[67] The error bar of the IP-EOM-CCSD method is larger than 1meV. However, the trend should remain the same. To confirm this, we have calculated the ionization potential (IP) for both systems using CCSD(T) method. The IP values are 71.81 eV and 71.18 eV for Li^+-H_2O and Li^+-NH_3 with partial inclusion of triples, respectively. We hope that the qualitative trend for decay width will be similar. Hence concluding that the Li^+-NH_3 decays faster than the Li^+-H_2O should remain the same.

Table 2: Effect of different molecular surroundings on ETMD process for Li 1s state in Li^+-H_2O and Li^+-NH_3 using aug-cc-pVTZ+1f basis set.

System	Energy (eV)	Width (meV)	lifetime(fs)
$Li^+ - H_2O$	71.89	7	96
$Li^+ - NH_3$	71.18	8	81

Li^+-water clusters: Effect of the increasing number of water molecules in surrounding on the ETMD process

We have used the aug-cc-pVDZ basis set for the Li^+-water dimer and trimer. The CAP box size used for the dimer is $C_x = 8$ a.u; $C_y = C_z = 5$ a.u. and $C_x = C_y = 10$ a.u; $C_z = 5$ a.u for the trimer. The Li^+ ion is a good example to study the ETMD process since it has only core electrons. Therefore, ICD and Auger decay process can not take place in this system.

If the Li^+-water cluster is ionized by removing an electron from the 1s subshell of the Li^+ ion, then the molecule relaxes via the ETMD process. The ETMD process of $Li^{2+}(1s^{-1}2s^{-1})$ state in Li^+-water clusters can be described as follows. After removing an electron from the 1s orbital of Li^+ ion in Li^+-H_2O (i.e. formation of Li^{2+}-H_2O), the 1s vacancy of $Li^{2+}(1s^{-1}2s^{-1})$ ion is filled up by a 2p outer valence electron of the oxygen atom of one of the water molecules. Then the released energy emits a secondary outer valence electron from the same water molecule or another water molecule. Therefore, the final state (Li^+-H_2O^{2+} or H_2O^+-Li^+-H_2O^+) of the ETMD process is a double ionized state (with respect to our initial system, i.e. Li^+-H_2O). The Li^+-H_2O^{2+} final state is produced via an ETMD(2) process, where both the positive charges are present on one water molecule. The H_2O^+-Li^+-H_2O^+ double ionized final state (with respect to our initial system, i.e. Li^+-H_2O) is produced via ETMD(3). The ETMD channel is open for the 1s ionized state of Li^+ ion because the energy of the $Li^{2+}(1s^{-1}2s^{-1})$ state lies above the double ionized final states (i.e. Li^+-H_2O^{2+} or H_2O^+-Li^+-H_2O^+). Thus, the positively charged water molecules will repel the positively charged Lithium ion leading to a Coulomb explosion. The different variants of ETMD (i.e. ETMD(2) or ETMD(3)) may be possible with an increasing number of water molecules surrounding

the Li^+ ion. The 1s ionization energy of the Li^+ ion in Li^+-water cluster varies from 72.35 to 67.45 eV depending on the number of water molecules present in the surroundings of Li^+ ion. Here, we have calculated the lifetime of 1s ionized state of Li^+ ion in various Li^+-water clusters.

In figure-3, we have plotted the decay values for the Li^+-$(H_2O)_n$;n=1,3 system. In this case, we have used the aug-cc-pVDZ basis set for the study. As we move from the monomer to the trimer, the decay position reduces from 72.35 eV to 67.45 eV. On the other hand, the decay width increases from 11 meV to 63 meV. There are two factors that can affect the decay width: first, the bond distance between the Li^+ and H_2O molecules and second, the number of surrounding water molecules. The bond length does not seem to have much effect as we move from the monomer (1.867 Å) to the dimer (1.86 Å). Therefore, the number of decay channels play a significant role in increasing the decay width as we move from monomer to dimer. From figure-3, we have noticed that the decay width increases nonlinearly. The possible reason for the nonlinear growth of the decay width is that the number of decay channels increases nonlinearly with an increasing number of water molecules surrounding the Li^+ ion. Cederbaum and Müller[26] have studied Li^+-H_2O with up to five water molecules using a perturbation theory ansatz with SCF integrals. They estimated lifetimes in the range of 100-20 fs. Our results give the decay time in the range from 60 fs to 10 fs from monomer to trimer in the aug-cc-pVDZ basis.[65] In the aug-cc-pVTZ basis set,[67] we obtained a lifetime of 98 fs which is in good agreement with the Cederbaum and Müller. See reference[72] for details of the IP and DIP spectra of the Li^+-$(H_2O)_n$ complex.

Na^+-water cluster: Effect of distance and increasing number of water molecules on the ICD process

The 2s ionized state of the Na atom in the Na^+-H_2O system can relax via the ICD process. The ICD process of the 2s ionized state of the Na atom in the Na^+-H_2O system can be described as follows: after removing an electron from the 2s subshell of Na atom, the 2s
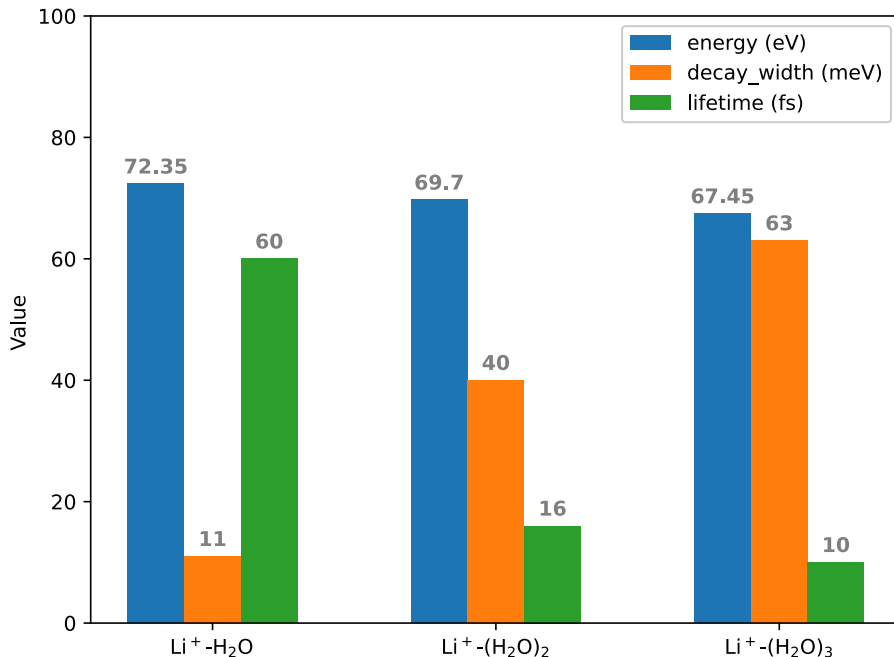
Figure 3: Effect of the increased number of surrounding water molecules on ETMD process using an aug-cc-pVDZ basis set.

vacancy of the Na atom in the Na^{2+}-H_2O is filled up by a 2p outer valence electron of the Na atom. Then the released energy is transferred to the neighbouring H_2O molecule which emits a secondary electron. Therefore, the final state of the ICD process is characterized by the Na^{2+} $(2p^{-1}3s^{-1})$ $O^{+}H_2$ $(2p^{-1})$ triple ionized state. Energetically, the ICD process is possible in the Na^{+}-H_2O system because the energy of the 2s ionized state of the Na atom lies above the energy of the Na^{2+} $(2p^{-1}3s^{-1})$ $O^{+}H_2(2p^{-1})$ final state.

The decay of the Sodium 2s state in the Na^{+}-H_2O system is studied in a modified maug-cc-pV(T+d)Z[73] basis set and augmented by 3s3p1d functions for Oxygen atom only(taken from the basis set exchange library,[74] then modified) for sodium and oxygen and cc-pVDZ[65] for hydrogen. The detailed basis set used for the system is described in supporting information. To see the effect of bond length on the decay width, we have studied the Na^{+}-water system for various bond lengths, i.e. 2.24988 $\mathring{A}$ to 5.0 $\mathring{A}$ between the sodium and the oxygen atom. The geometry was optimized using the CCSD method in the aug-cc-pVDZ basis[65] and the bond distance between sodium and oxygen was found to be 2.24988 $\mathring{A}$. Thus, we have used

this bond distance. The CAP box size used in our calculation is $C_x = 8.7$, $C_y = 6.5$ and $C_z = 5.0$ a.u. Fig 4 summarizes the results for various bond lengths. We know from equation 2 that the decay width and lifetime of a temporary bound state (TBS) are inversely proportional to each other. We observe that the lifetime increases rapidly as bond length increases or the decay width rapidly decreases with an increase in the bond length. A sharp change in decay width from 251 meV (2.6 fs) at 2.24988 $\mathring{A}$ to 142 meV (4.6 fs) at 2.29 $\mathring{A}$ is observed. Then it saturates at 33 meV (20 fs) at 5.0$\mathring{A}$. It may become bound with a further increase in the bond length. We also report the Fano-ADC[29] results at 2.30 Å. The basis set used in that calculation is cc-pCVTZ+2s2p2d1f KBJ[66] for sodium and oxygen and cc-pVTZ+1s1p1d KBJ[66] for hydrogen. The lifetime of 7 fs was reported using the Fano-ADC method. The experimental[75] value of the decay time of the Na 2s state is 3.1 fs. Our results predict the decay time to be 2.6 fs at the equilibrium bond length which shows good agreement with the experimental value.
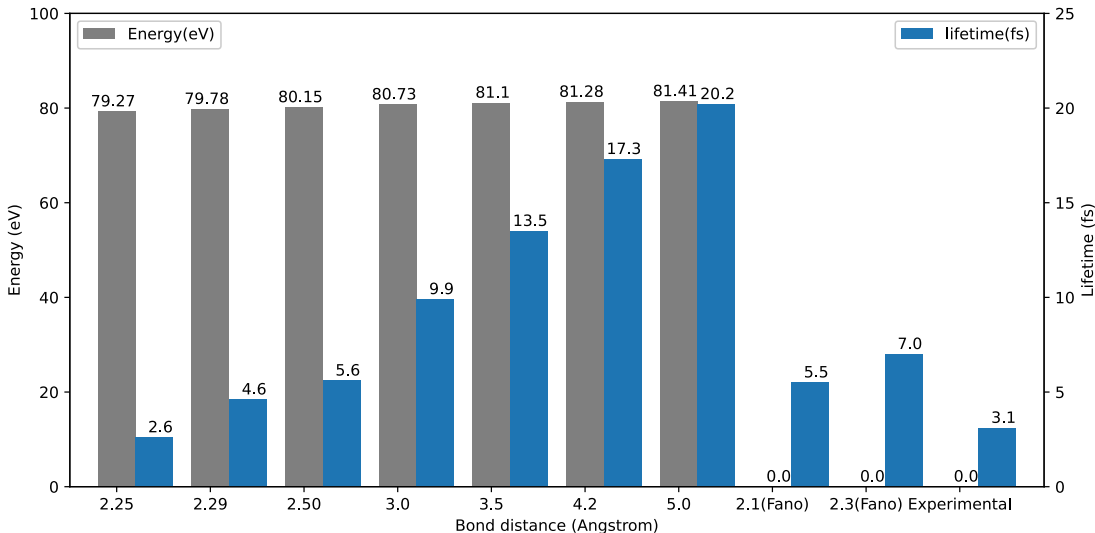
Figure 4: Effect of bond length on ICD process for the 2s state of Na in Na$^+$-H$_2$O using maug-cc-pV(T+d)Z basis set.

To see the effect of the increased number of surrounding molecules on the decay width in the ICD process, we also studied the Na$^+$-water dimer. The optimized geometry was obtained using the B3LYP functional[68–71] and the 6-311++g(3d,2p) basis set[76] in the Gaussian09[64]

Table 3: Different decay process in different systems: Auger decay in K^+-H_2O, ICD in Na^+-$(H_2O)_n$ and ETMD in Li^+-$(H_2O)_n$ (where n=1,2).

Basis	System	Energy (eV)	Width in meV (fs)
maug-cc-pV(T+d)Z@	Li^+-H_2O	71.81	7.64 (86)
maug-cc-pV(T+d)Z@	Li^+-$(H_2O)_2$	69.03	16.12 (40.8)
maug-cc-pV(T+d)Z**	Na^+-H_2O	79.49	129 (5.1)
maug-cc-pV(T+d)Z**	Na^+-$(H_2O)_2$	78.19	305 (2.1)
aug-cc-pVDZ-X2C	K^+-H_2O (2s)	396	423 (1.5) 278 (2.4)*
aug-cc-pVDZ-X2C	K^+-H_2O (2p)	315	74.86 (8.8) 246 (2.7)*

* represents the 2nd decay value that we have observed.
** represents the maug-cc-pV(T+d)Z + 3s3p1d on O atom in Spherical basis.
@ represents the maug-cc-pV(T+d)Z + 3s3p1d on O atom in Cartesian basis.

software package. The CAP box size used for the Na^+-water system in our calculation is $C_x = 12$, $C_y = 7$ and $C_z = 7$ a.u. We have used a spherical basis set for the Na^+-water dimer due to scaling of the CC equations (i.e. in a cartesian basis, the Na^+-water dimer is computationally very expensive). To compare Na^+-$(H_2O)_2$ with Na^+-H_2O, we again run Na^+-H_2O in a spherical basis set. The bond distance between Sodium and Oxygen is 2.2453 $\mathring{A}$ in Na^+-$(H_2O)_2$ and 2.24988 $\mathring{A}$ in Na^+-H_2O. The decay width of the 2s state of Sodium in Na^+-$(H_2O)_2$ is 305 meV (2.1 fs) compared to 129 meV (5.1 fs) in Na^+-H_2O.

Auger Decay process for the 2s and 2p ionized states of K in K^+-water

The 2s and 2p ionized states of the K atom in the K^+-H_2O can relax via the Auger process. In our calculations, we have used the optimized geometry for K^+-H_2O obtained using the B3LYP functional[68–71] and the 6-311++g(3d,2p) basis set[77] in the Gaussian09[64] software package. For the computation of the decay width, we have employed the aug-cc-pVDZ-X2C basis set[78] for potassium, aug-cc-pVDZ[65] for oxygen and the cc-pVDZ basis set[65] for hydrogen. The results for the 2s and 2p ionized states are presented in Table-3 along with Li^+-$(H_2O)_n$ and Na^+-$(H_2O)_n$; n=1,2. Here, for the Li^+-$(H_2O)_n$; n=1,2, we have used the

maug-cc-pV(T+d)Z[73]+ 3s3p1d basis set on Oxygen while for Li we have used maug-cc-pV(T+d)Z basis set[73] to maintain consistency. The CAP box size used for K^+-water system in our calculation is $C_x = 7$, $C_y = 4$ and $C_z = 4$ a.u. In the case of the K^+-H_2O system, we observed two stationary points on the η trajectory indicating decay through a cascade mechanism. Experimentally, a similar kind of two stationary points (cascade decay type effect) was observed.[79] The η trajectory shows only one stationary point for the other two systems (Li^+-H_2O, Na^+-H_2O).

The Auger process of the (2s, 2p) ionized state of the K atom in K^+-H_2O ($4s^{-1}$) can be rationalized as follows: After removing an electron from the 2s or 2p subshell of the K atom in K^+-H_2O (formation of K^{2+}-H_2O)($2s^{-1}$ $4s^{-1}$ or $2p^{-1}$ $4s^{-1}$), the 2s or 2p vacancy is filled up by a 3p or 3s outer valence electron of the K atom. Then the released energy is used to knock out another secondary outer valence electron from the 3p or 3s subshell of the K atom (formation of K^{3+}-H_2O). This two-hole state (K^{3+}($3p^{-2}$ $4s^{-1}$)H_2O or K^{3+}($3p^{-1}$ $3s^{-1}$ $4s^{-1}$)H_2O or K^{3+}($3s^{-2}$ $4s^{-1}$)H_2O) (which is with respect to our initial system K^+-H_2O) is unstable and further relax via another decay process which is a three-hole state. Energetically the Auger process will be viable if the energy of the 2s or 2p ionized state of the K atom lies above the triple ionized final states. The calculation of the three-hole state is beyond the scope of this paper.

The Auger decay width for the 2p ionized state is 75 meV (i.e. 8.8 fs) which undergoes further decay with a decay width of 246 meV corresponding to a lifetime of 2.7 fs. Similarly, the Auger decay width for the 2s ionized state is 423 meV with a lifetime of 1.5 fs which undergoes further decay with a decay width of 278 meV corresponding to a lifetime of 2.4 fs. Pokapanich et al.[16] have studied the Auger decay in potassium chloride surrounded by water molecules.

Polarized Surrounding effect on ETMD and ICD

We have studied the Li^+-water and Na^+-water in the gaseous and aqueous medium to see the effect of a polarized surrounding on the decay width in the ETMD and ICD processes, respectively. We have used the PCM model[63] for the aqueous phase, where water is the solvent. The bond distance and CAP box size were kept identical for the gaseous and aqueous phases. The results are presented in Table 4. For the Li^+-water 1s state, the decay position remains almost identical; however, the decay width changes from 12 meV (56 fs) for the gaseous medium to 9.7 meV (67 fs) for the aqueous medium. The decay is slower in the aqueous medium compared to the gaseous medium. A similar trend was observed for the Na^+-water's 2s state and the decay width changes from 143 meV (4.6) for the gaseous medium to 108 meV (6 fs) for the aqueous medium. The slow decay in the aqueous medium is due to the polarization provided by the medium which makes the ionized state more stable than the gaseous medium.

Table 4: Polarization effect on decay width in ETMD and ICD processes for X^+-H_2O system (X = Li, Na).

Basis	System	medium	Energy (eV)	Width in meV(fs)
aug-cc-pVDZ +F(O)	$Li^+ - H_2O$	GAS	72.36	12 (56)
aug-cc-pVDZ+F(O)	$Li^+ - H_2O$	PCM	72.3	9.7 (67)
m-aug-cc-PV(T+d)Z	$Na^+ - H_2O$	GAS	79.78	143 (4.6)
m-aug-cc-PV(T+d)Z	$Na^+ - H_2O$	PCM	79.73	108 (6.0)

Conclusions

This paper has used the CAP-IP-EOM-CCSD method to study the various decay processes in microsolvated alkali metal ions i.e. Li^+, Na^+ and K^+. The CAP-IP-EOM-CCSD method is used for the first time to explore the ETMD lifetimes for the Li 1s state in Li^+-H_2O clusters. It is observed that the decay widths are sensitive to the bond length, surrounding atoms, medium (gas or liquid) and the number of neighboring molecules. We have studied

the effect of all these parameters on the decay width of Li^+-H_2O and Na^+-H_2O clusters.

We have studied the decay of 1s, 2s, and both 2s and 2p states in Li^+, Na^+ and K^+ with water, respectively. The Li 1s state undergoes ETMD whereas the Na 2s state decays via ICD. The K 2s and 2p states undergo Auger decay. To study the impact of different molecular environments, the 1s ionized state of the Li atom was studied in Li^+-NH_3 and Li^+-H_2O. Since water and ammonia are isoelectronic, it will be interesting to study the effect of the environment on the decay width. We found that decay is faster in Li^+-NH_3 (81 fs) than in Li^+-H_2O (96 fs). The possible explanation for this could be, first, the higher electronegativity of oxygen than nitrogen, making electron transfer more difficult than nitrogen. Second, the location of the lone pair. In Li^+-NH_3, it is between Li^+ and nitrogen, whereas in Li^+-H_2O, it is perpendicular to the molecular plane. Because of the directional nature of p-orbitals and the orientation of the lone pair toward lithium, electron transfer is much faster in the case of ammonia than water (See Figure-2 for details).

We have studied the ETMD lifetime for the 1s ionized state of the Li atom in the Li^+-$(H_2O)_n$ (n=1,3) system to see the effect of the number of water molecules on the decay. The lifetime obtained for the Li^+-$(H_2O)_n$ system is 60 fs, 16 fs and drops further to 10 fs as n increases from 1 to 3. As a characteristic feature of ETMD, the lifetime decreases strongly with an increasing number of neighbours. This is due to a nonlinear increase in the number of decay channels with an increasing number of surrounding atoms.

To see the effect of bond length on the decay width for the ICD process, we studied the 2s ionized state of Na atom in Na^+-H_2O at various bond lengths, i.e. 2.2489 $\mathring{A}$ to 5.0 $\mathring{A}$. We observe that as the bond length increases, the decay width reduces and the lifetime increases from 2.6 fs at 2.24 $\mathring{A}$ to 20 fs at 5.0 $\mathring{A}$. A similar trend was observed using the Fano ADC method.[29] The authors report a lifetime of 5.5 fs at 2.21 $\mathring{A}$ and 7 fs at 2.30 $\mathring{A}$. Our results for sodium 2s state are in good agreement with the experiment[75] and the Fano ADC[29] method. We have also investigated the ICD lifetime for the 2s ionized state of the Na atom in the Na^+-$(H_2O)_n$ (n=1,2) systems to study the effect of increased water

20

molecules in the surrounding on ICD. The computed ICD lifetime for the Na^+-H_2O system is 5.1 fs, and it decreases strongly to 2.1 fs for the Na^+-$(H_2O)_2$ system. We have used a spherical Gaussian basis set here for monomer and dimer to have a proper comparison. The sensitivity of the decay width to the spherical or cartesian basis is also observed. We have investigated the Auger lifetime for the 2s and 2p ionized state of the K atom in the K^+-(H_2O) system. The computed Auger lifetimes for the 2s and 2p ionized states are 2.36 fs and 2.67 fs, respectively. The η trajectory indicates a cascade decay for the K^+-(H_2O) system. The Auger decay initiates another decay after a short-lived state leading to a more stable state. Since the Auger decay is a localized decay, we do not expect much change with bond length or number of neighbours.

To know the polarization effect on the ICD and ETMD processes, we studied the decay of the 1s state of the Li atom and the 2s state of Na in Li^+-(H_2O) and Na^+-(H_2O), respectively. We used the PCM model[63] in our study. In both cases, our results show that the polarization stabilizes the system, i.e. decay time is increased in the liquid phase compared to the gaseous phase. In this paper, we studied the decay width of alkali metal ions as a function of different molecular environments, increase of surrounding molecules in a system, bond distance, basis set and polarization of the medium.

Acknowledgement

Supporting Information Available

The data that support the findings of this study are available as supporting information submitted to ACS. Any further data will be available on request from corresponding authors.

References

(1) Auger, P. Sur l' effet Photoélectrique Composé. *J. Phys. Radium* **1925**, *6*, 205–208.

(2) Cederbaum, L. S.; Zobeley, J.; Tarantelli, F. Giant Intermolecular Decay and Fragmentation of Clusters. *Phys. Rev. Lett.* **1997**, *79*, 4778–4781.

(3) Santra, R.; Cederbaum, L. S. Non-Hermitian Electronic Theory and Applications to Clusters. *Phys. Rep.* **2002**, *368*, 1–117.

(4) Zobeley, J.; Santra, R.; Cederbaum, L. S. Electronic Decay in Weakly Bound Heteroclusters: Energy Transfer versus Electron Transfer. *J. Chem. Phys.* **2001**, *115*, 5076–5088.

(5) Scheit, S.; Averbukh, V.; Meyer, H.; Moiseyev, N.; Santra, R.; Sommerfeld, T.; Zobeley, J.; Cederbaum, L. S. On the Interatomic Coulombic Decay in the Ne Dimer. *J. Chem. Phys.* **2004**, *121*, 8393–8398.

(6) Vaval, N.; Cederbaum, L. S. Ab Initio Lifetimes in the Interatomic Coulombic Decay of Neon Clusters Computed with Propagators. *J. Chem. Phys.* **2007**, *126*, 164110.

(7) Ehara, M.; Sommerfeld, T. CAP/SAC-CI Method for Calculating Resonance States of Metastable Anions. *Chem. Phys. Lett.* **2012**, *537*, 107–112.

(8) Jahnke, T. Interatomic and Intermolecular Coulombic Decay: The Coming of Age Story. *J. Phys. B: At. Mol. Opt. Phys.* **2015**, *48*, 082001.

(9) Marburger, S.; Kugeler, O.; Hergenhahn, U.; Möller, T. Experimental Evidence for Interatomic Coulombic Decay in Ne Clusters. *Phys. Rev. Lett.* **2003**, *90*, 203401.

(10) Jahnke, T.; Czasch, A.; Schöffler, M. S.; Schössler, S.; Knapp, A.; Käsz, M.; Titze, J.; Wimmer, C.; Kreidi, K.; Grisenti, R. E.; Staudte, A.; Jagutzki, O.; Hergenhahn, U.; Schmidt-Böcking, H.; Dörner, R. Experimental Observation of Interatomic Coulombic Decay in Neon Dimers. *Phys. Rev. Lett.* **2004**, *93*, 163401.

(11) Öhrwall, G.; Tchaplyguine, M.; Lundwall, M.; Feifel, R.; Bergersen, H.; Rander, T.; Lindblad, A.; Schulz, J.; Peredkov, S.; Barth, S.; Marburger, S.; Hergenhahn, U.; Svensson, S.; Björneholm, O. Femtosecond Interatomic Coulombic Decay in Free Neon Clusters: Large Lifetime Differences between Surface and Bulk. *Phys. Rev. Lett.* **2004**, *93*, 173401.

(12) Santra, R.; Zobeley, J.; Cederbaum, L. S.; Moiseyev, N. Interatomic Coulombic Decay in Van Der Waals Clusters and Impact of Nuclear Motion. *Phys. Rev. Lett.* **2000**, *85*, 4490–4493.

(13) Sisourat, N.; Sann, H.; Kryzhevoi, N. V.; Kolorenč, P.; Havermeier, T.; Sturm, F.; Jahnke, T.; Kim, H. K.; Dörner, R.; Cederbaum, L. S. Interatomic Electronic Decay Driven by Nuclear Motion. *Phys. Rev. Lett.* **2010**, *105*, 173401.

(14) Stoychev, S. D.; Kuleff, A. I.; Cederbaum, L. S. On the Intermolecular Coulombic Decay of Singly and Doubly Ionized States of Water Dimer. *J. Chem. Phys.* **2010**, *133*, 154307.

(15) Thürmer, S.; Unger, I.; Slavíček, P.; Winter, B. Relaxation of Electronically Excited Hydrogen Peroxide in Liquid Water: Insights from Auger-Electron Emission. *J. Phys. Chem. C* **2013**, *117*, 22268–22275.

(16) Pokapanich, W.; Kryzhevoi, N. V.; Ottosson, N.; Svensson, S.; Cederbaum, L. S.; Öhrwall, G.; Björneholm, O. Ionic-Charge Dependence of the Intermolecular Coulombic

Decay Time-Scale for Aqueous Ions Probed by the Core-Hole Clock. *J. Am. Chem. Soc.* **2011**, *133*, 13430–13436.

(17) Fasshauer, E.; Förstel, M.; Mucke, M.; Arion, T.; Hergenhahn, U. Theoretical and Experimental Investigation of Electron Transfer Mediated Decay in ArKr Clusters. *Chem. Phys.* **2017**, *482*, 226–238.

(18) Förstel, M.; Mucke, M.; Arion, T.; Bradshaw, A. M.; Hergenhahn, U. Autoionization Mediated by Electron Transfer. *Phys. Rev. Lett.* **2011**, *106*, 033402.

(19) Yan, S.; Zhang, P.; Ma, X.; Xu, S.; Li, B.; Zhu, X. L.; Feng, W. T.; Zhang, S. F.; Zhao, D. M.; Zhang, R.; Guo, D.; Liu, H. P. Observation of Interatomic Coulombic Decay and Electron Transfer Mediated Decay in High Energy Electron Impact Ionization of Ar_2. *Phys. Rev. A* **2013**, *88*, 042712.

(20) Sakai, K.; Stoychev, S.; Ouchi, T.; Higuchi, I.; Schöffler, M.; Mazza, T.; Fukuzawa, H.; Nagaya, K.; Yao, M.; Tamenori, Y.; Kuleff, A. I.; Saito, N.; Ueda, K. Electron Transfer Mediated Decay and Interatomic Coulombic Decay from the Triply Ionized States in Argon Dimers. *Phys. Rev. Lett.* **2011**, *106*, 033401.

(21) LaForge, A. C.; Stumpf, V.; Gokhberg, K.; von Vangerow, J.; Stienkemeier, F.; Kryzhevoi, N. V.; O'Keeffe, P.; Ciavardini, A.; Krishnan, S. R.; Coreno, M.; Prince, K. C.; Richter, R.; Moshammer, R.; Pfeifer, T.; Cederbaum, L. S.; Mudrich, M. Enhanced Ionization of Embedded Clusters by Electron-Transfer-Mediated Decay in Helium Nanodroplets. *Phys. Rev. Lett.* **2016**, *116*, 203001.

(22) Ghosh, A.; Cederbaum, L. S.; Gokhberg, K. Electron Transfer Mediated Decay in $HeLi_2$ Cluster: Potential Energy Surfaces and Decay Widths. *J. Chem. Phys.* **2019**, *150*, 164309.

(23) Kryzhevoi, N. V.; Averbukh, V.; Cederbaum, L. S. High Activity of Helium Droplets Following Ionization of Systems Inside Those Droplets. *Phys. Rev. B* **2007**, *76*, 094513.

(24) Ben Ltaief, L.; Shcherbinin, M.; Mandal, S.; Krishnan, S. R.; Richter, R.; Pfeifer, T.; Bauer, M.; Ghosh, A.; Mudrich, M.; Gokhberg, K.; LaForge, A. C. Electron Transfer Mediated Decay of Alkali Dimers Attached to He Nanodroplets. *Phys. Chem. Chem. Phys.* **2020**, *22*, 8557–8564.

(25) Unger, I.; Seidel, R.; Thürmer, S.; Pohl, M. N.; Aziz, E. F.; Cederbaum, L. S.; Muchová, E.; Slavíček, P.; Winter, B.; Kryzhevoi, N. V. Observation of Electron Transfer Mediated Decay in Aqueous Solution. *Nat. Chem.* **2017**, *9*, 708–714.

(26) Müller, I. B.; Cederbaum, L. S. Electronic Decay Following Ionization of Aqueous Li$^+$ Microsolvation Clusters. *J. Chem. Phys.* **2005**, *122*, 094305.

(27) Stumpf, V.; Gokhberg, K.; Cederbaum, L. S. The Role of Metal Ions in X-ray Induced Photochemistry. *Nat. Chem.* **2016**, *8*, 237–241.

(28) Ghosh, A.; Cederbaum, L. S.; Gokhberg, K. Signature of the Neighbor's Quantum Nuclear Dynamics in the Electron Transfer Mediated Decay Spectra. *Chem. Sci.* **2021**, *12*, 9379–9385.

(29) Stumpf, V.; Brunken, C.; Gokhberg, K. Impact of Metal Ion's Charge on the Interatomic Coulombic Decay Widths in Microsolvated Clusters. *J. Chem. Phys.* **2016**, *145*, 104306.

(30) Brun, E.; Cloutier, P.; Sicard-Roselli, C.; Fromm, M.; Sanche, L. Damage Induced to DNA by Low-Energy (0-30 eV) Electrons under Vacuum and Atmospheric Conditions. *J. Phys. Chem. B* **2009**, *113*, 10008–10013.

(31) Alizadeh, E.; Orlando, T. M.; Sanche, L. Biomolecular Damage Induced by Ionizing Radiation: The Direct and Indirect Effects of Low-Energy Electrons on DNA. *Annu. Rev. Phys. Chem.* **2015**, *66*, 379–398.

(32) Ren, X.; Wang, E.; Skitnevskaya, A. D.; Trofimov, A. B.; Gokhberg, K.; Dorn, A.

Experimental Evidence for Ultrafast Intermolecular Relaxation Processes in Hydrated Biomolecules. *Nat. Phys.* **2018**, *14*, 1062–1066.

(33) Sussman, F.; Weinstein, H. On the Ion Selectivity in Ca-Binding Proteins: The Cyclo(-L-Pro-Gly-)3 Peptide as a Model. *Proc. Natl. Acad. Sci. USA* **1989**, *86*, 7880–7884.

(34) Dill, K. A. Dominant Forces in Protein Folding. *Biochemistry* **1990**, *29*, 7133–7155.

(35) Forrest, M. D. The Sodium-Potassium Pump is an Information Processing Element in Brain Computation. *Front. Physiol.* **2014**, *5*, 472.

(36) Clausen, M. V.; Hilbers, F.; Poulsen, H. The Structure and Function of the Na,K-ATPase Isoforms in Health and Disease. *Front. Physiol.* **2017**, *8*, 371.

(37) Ghosh, A.; Vaval, N. Geometry-Dependent Lifetime of Interatomic Coulombic Decay using Equation-of-Motion Coupled Cluster Method. *J. Chem. Phys.* **2014**, *141*, 234108.

(38) Ghosh, A.; Pal, S.; Vaval, N. Study of Interatomic Coulombic Decay of $Ne(H2O)_n$ (n=1,3) Clusters Using Equation-of-Motion Coupled Cluster Method. *J. Chem. Phys.* **2013**, *139*, 064112.

(39) Ghosh, A.; Vaval, N.; Pal, S.; Bartlett, R. J. Complex Absorbing Potential Based Equation-of-Motion Coupled Cluster Method for the Potential Energy Curve of CO_2^- Anion. *J. Chem. Phys.* **2014**, *141*, 164113.

(40) Jagau, T. C.; Zuev, D.; Bravaya, K. B.; Epifanovsky, E.; Krylov, A. I. A Fresh Look at Resonances and Complex Absorbing Potentials: Density Matrix-Based Approach. *J. Phys. Chem. Lett.* **2014**, *5*, 310–315.

(41) Zuev, D.; Jagau, T. C.; Bravaya, K. B.; Epifanovsky, E.; Shao, Y.; Sundstrom, E.; Head-Gordon, M.; Krylov, A. I. Complex Absorbing Potentials within EOM-CC Family of Methods: Theory, Implementation, and Benchmarks. *J. Chem. Phys.* **2014**, *141*, 024102.

(42) Jagau, T. C.; Krylov, A. I. Complex Absorbing Potential Equation-of-Motion Coupled-Cluster Method Yields Smooth and Internally Consistent Potential Energy Surfaces and Lifetimes for Molecular Resonances. *J. Phys. Chem. Lett.* **2014**, *5*, 3078–3085.

(43) Sajeev, Y.; Ghosh, A.; Vaval, N.; Pal, S. Coupled Cluster Methods for Autoionisation Resonances. *Int. Rev. Phys. Chem.* **2014**, *33*, 397–425.

(44) Bartlett, R. J.; Musiał, M. Coupled Cluster Theory in Quantum Chemistry. *Rev. Mod. Phys.* **2007**, *79*, 291–352.

(45) Lyakh, D. I.; Musiał, M.; Lotrich, V. F.; Bartlett, R. J. Multireference Nature of Chemistry: The Coupled Cluster View. *Chem. Rev.* **2012**, *112*, 182–243.

(46) Nooijen, M.; Bartlett, R. J. Equation-of-Motion Coupled Cluster Method for Electron Attachment. *J. Chem. Phys.* **1995**, *102*, 3629–3647.

(47) Stanton, J. F.; Bartlett, R. J. The Equation-of-Motion Coupled Cluster Method. A Systematic Biorthogonal Approach to Molecular Excitation Energies, Transition Probabilities, and Excited State Properties. *J. Chem. Phys.* **1993**, *98*, 7029–7039.

(48) Nooijen, M.; Bartlett, R. J. Similarity Transformed Equation-of-Motion Coupled-Cluster Theory: Details, Examples, and Comparisons. *J. Chem. Phys.* **1997**, *107*, 6812–6830.

(49) Musiał, M.; Bartlett, R. J. Charge Transfer Separability and Size Extensivity in the Equation-of-Motion Coupled Cluster Method: EOM-CCx. *J. Chem. Phys.* **2011**, *134*, 034106.

(50) Musiał, M.; Kucharski, S. A.; Bartlett, R. J. Equation-of-Motion Coupled Cluster Method with Full Inclusion of the Connected Triple Excitations for Ionized States: IP-EOM-CCSDT. *J. Chem. Phys.* **2003**, *118*, 1128–1136.

(51) Siegert, A. J. F. On the Derivation of the Dispersion Formula for Nuclear Reactions. *Phys. Rev.* **1939**, *56*, 750–752.

(52) Moiseyev, N.; Corcoran, C. Autoionizing States of H_2 and H_2^- using the Complex-Scaling Method. *Phys. Rev. A* **1979**, *20*, 814–817.

(53) Moiseyev, N. Quantum Theory of Resonances: Calculating Energies, Widths and Cross-Sections by Complex Scaling. *Phys. Rep.* **1998**, *302*, 212–293.

(54) Moiseyev, N. Derivations of Universal Exact Complex Absorption Potentials by the Generalized Complex Coordinate Method. *J. Phys. B: At. Mol. Opt. Phys.* **1998**, *31*, 1431–1441.

(55) Sommerfeld, T.; Riss, U. V.; Meyer, H. D.; Cederbaum, L. S.; Engels, B.; Suter, H. U. Temporary Anions - Calculation of Energy and Lifetime by Absorbing Potentials: The Resonance. *J. Phys. B: At. Mol. Opt. Phys.* **1998**, *31*, 4107–4122.

(56) Jolicard, G.; Austin, E. J. Optical Potential Stabilisation Method for Predicting Resonance Levels. *Chem. Phys. Lett.* **1985**, *121*, 106–110.

(57) Riss, U. V.; Meyer, H. D. Calculation of Resonance Energies and Widths using the Complex Absorbing Potential Method. *J. Phys. B: At. Mol. Opt. Phys.* **1993**, *26*, 4503–4535.

(58) Muga, J.; Palao, J.; Navarro, B.; Egusquiza, I. Complex Absorbing Potentials. *Phys. Rep.* **2004**, *395*, 357–426.

(59) Riss, U. V.; Meyer, H. D. The Transformative Complex Absorbing Potential Method: A Bridge between Complex Absorbing Potentials and Smooth Exterior Scaling. *J. Phys. B: At. Mol. Opt. Phys.* **1998**, *31*, 2279–2304.

(60) Sajeev, Y.; Santra, R.; Pal, S. Correlated Complex Independent Particle Potential for Calculating Electronic Resonances. *J. Chem. Phys.* **2005**, *123*, 204110.

(61) Sajeev, Y.; Pal, S. A General Formalism of the Fock Space Multireference Coupled Cluster Method for Investigating Molecular Electronic Resonances. *Mol. Phys.* **2005**, *103*, 2267–2275.

(62) Ghosh, A.; Karne, A.; Pal, S.; Vaval, N. CAP/EOM-CCSD Method for the Study of Potential Curves of Resonant States. *Phys. Chem. Chem. Phys.* **2013**, *15*, 17915–17921.

(63) Tomasi, J.; Mennucci, B.; Cammi, R. Quantum Mechanical Continuum Solvation Models. *Chem. Rev.* **2005**, *105*, 2999–3094.

(64) Frisch, M. J.; Trucks, G. W.; Schlegel, H. B.; Scuseria, G. E.; Robb, M. A.; Cheeseman, J. R.; Scalmani, G.; Barone, V.; Mennucci, B.; Petersson, G. A.; Nakatsuji, H.; Caricato, M.; Li, X.; Hratchian, H. P.; Izmaylov, A. F.; Bloino, J.; Zheng, G.; Sonnenberg, J. L.; Hada, M.; Ehara, M.; Toyota, K.; Fukuda, R.; Hasegawa, J.; Ishida, M.; Nakajima, T.; Honda, Y.; Kitao, O.; Nakai, H.; Vreven, T.; Montgomery, J., J. A.; Peralta, J. E.; Ogliaro, F.; Bearpark, M.; Heyd, J. J.; Brothers, E.; Kudin, K. N.; Staroverov, V. N.; Kobayashi, R.; Norm and, J.; Raghavachari, K.; Rendell, A.; Burant, J. C.; Iyengar, S. S.; Tomasi, J.; Cossi, M.; Rega, N.; Millam, J. M.; Klene, M.; Knox, J. E.; Cross, J. B.; Bakken, V.; Adamo, C.; Jaramillo, J.; Gomperts, R.; Stratmann, R. E.; Yazyev, O.; Austin, A. J.; Cammi, R.; Pomelli, C.; Ochterski, J. W.; Martin, R. L.; Morokuma, K.; Zakrzewski, V. G.; Voth, G. A.; Salvador, P.; Dannenberg, J. J.; Dapprich, S.; Daniels, A. D.; Farkas, Ã.; Foresman, J. B.; Ortiz, J. V.; Cioslowski, J.; Fox, D. J. *Gaussian-09*, Revision C.01 ed.; Gaussian Inc.: Wallingford CT, 2009.

(65) Dunning, T. H. Gaussian Basis Sets for Use in Correlated Molecular Calculations. I. The Atoms Boron Through Neon and Hydrogen. *J. Chem. Phys.* **1989**, *90*, 1007–1023.

(66) Kaufmann, K.; Baumeister, W.; Jungen, M. Universal Gaussian Basis Sets for an Opti-

mum Representation of Rydberg and Continuum Wavefunctions. *J. Phys. B: At. Mol. Opt. Phys.* **1989**, *22*, 2223–2240.

(67) Kendall, R. A.; Dunning, T. H.; Harrison, R. J. Electron Affinities of the First-Row Atoms Revisited. Systematic Basis Sets and Wave Functions. *J. Chem. Phys.* **1992**, *96*, 6796–6806.

(68) Becke, A. D. Density-Functional Thermochemistry. III. The Role of Exact Exchange. *J. Chem. Phys.* **1993**, *98*, 5648–5652.

(69) Lee, C.; Yang, W.; Parr, R. G. Development of the Colle-Salvetti Correlation-Energy Formula into a Functional of the Electron Density. *Phys. Rev. B* **1988**, *37*, 785–789.

(70) Stephens, P. J.; Devlin, F. J.; Chabalowski, C. F.; Frisch, M. J. Ab Initio Calculation of Vibrational Absorption and Circular Dichroism Spectra Using Density Functional Force Fields. *J. Phys. Chem.* **1994**, *98*, 11623–11627.

(71) Vosko, S. H.; Wilk, L.; Nusair, M. Accurate Spin-Dependent Electron Liquid Correlation Energies for Local Spin Density Calculations: A Critical Analysis. *Can. J. Phys.* **1980**, *58*, 1200–1211.

(72) Müller, I. B.; Cederbaum, L. S.; Tarantelli, F. Microsolvation of Li^+ in Water Analyzed by Ionization and Double Ionization. *J. Phys. Chem. A* **2004**, *108*, 5831–5844.

(73) Papajak, E.; Leverentz, H. R.; Zheng, J.; Truhlar, D. G. Efficient Diffuse Basis Sets: cc-pVxZ+ and maug-cc-pVxZ. *J. Chem. Theory Comput.* **2009**, *5*, 3330–3330.

(74) Pritchard, B. P.; Altarawy, D.; Didier, B.; Gibson, T. D.; Windus, T. L. New Basis Set Exchange: An Open, Up-to-Date Resource for the Molecular Sciences Community. *J. Chem. Inf. Model.* **2019**, *59*, 4814–4820.

(75) Öhrwall, G.; Ottosson, N.; Pokapanich, W.; Legendre, S.; Svensson, S.; Björneholm, O.

Charge Dependence of Solvent-Mediated Intermolecular Coster-Kronig Decay Dynamics of Aqueous Ions. *J. Phys. Chem. B* **2010**, *114*, 17057–17061.

(76) McLean, A. D.; Chandler, G. S. Contracted Gaussian Basis Sets for Molecular Calculations. I. Second Row Atoms, Z=11-18. *J. Chem. Phys.* **1980**, *72*, 5639–5648.

(77) Blaudeau, J.-P.; McGrath, M. P.; Curtiss, L. A.; Radom, L. Extension of Gaussian-2 (G2) Theory to Molecules Containing Third-Row Atoms K and Ca. *J. Chem. Phys.* **1997**, *107*, 5016–5021.

(78) Hill, J. G.; Peterson, K. A. Gaussian Basis Sets for Use in Correlated Molecular Calculations. XI. Pseudopotential-Based and All-Electron Relativistic Basis Sets for Alkali Metal (K-Fr) and Alkaline Earth (Ca-Ra) Elements. *J. Chem. Phys.* **2017**, *147*, 244106.

(79) Pokapanich, W.; Bergersen, H.; Bradeanu, I. L.; Marinho, R. R. T.; Lindblad, A.; Legendre, S.; Rosso, A.; Svensson, S.; , O. B.; Tchaplyguine, M.; , G. Ã.; Kryzhevoi, N. V.; Cederbaum, L. S. Auger Electron Spectroscopy as a Probe of the Solution of Aqueous Ions. *J. Am. Chem. Soc.* **2009**, *131*, 7264–7271.

Graphical TOC Entry